Quantum chaos, localized states and clustering in excited spectra of Jahn-Teller models

Eva Majerníková [a, b] S. Shpyrko [b]

[a] Institute of Physics, Slovak Academy of Sciences, Dúbravská cesta 9, SK-84 511 Bratislava, Slovak Republic

[b] Department of Theoretical Physics, Palacký University, Tř. 17. listopadu 50, CZ-77207 Olomouc, Czech Republic

We studied complex spectra of spin-two boson systems represented by E⊗e and E⊗(b_1+b_2) Jahn-Teller models. For E⊗e, at particular rotation quantum numbers we found a coexistence of up to three regions of the spectra, (i) the dimerized region of long-range ordered (extended) pairs of oscillating levels, (ii) the short-range ordered (localized) "kink lattice" of avoiding levels, and (iii) the intermediate region of kink nucleation with variable range of ordering. This structure appears above certain critical line as a function of interaction strength. The level clustering and level avoiding generic patterns reflect themselves in several intermittent regions between up-to three branches of spectral entropies. Linear scaling behavior of the widths of curvature probability distributions provides the conventionally adopted indication for the presence of quantum chaos. The mapping onto classical integrable Calogero-Moser gas provided useful insight into the complex level dynamics, including the soliton collisions representing the level avoidings and, in a range of model parameters, a novel view on the notion of quantum chaos formulated in terms of quantum numbers via the logistic equation. We found that apart from two limiting cases of $E\otimes(b_1+b_2)$ model ($E\otimes e$ and Holstein model) the distribution of nearest neighbor spacings of this model is rather stable as to the change of parameters and different from Wigner one. This limiting distribution assumably shows scaling $\sim\sqrt{S}$ at small S and resembles the semi-Poisson law $P(S)=4S\exp(-2S)$ at $S\geq 1$. The latter is believed to be universal and characteristic, e.g. at the transition between metal and insulator phases.

1. Introduction

The results of intensive research in quantum mechanics show ([1]-[3]) that the smooth wave-like quantum world contains elements of quantum complexity and that symptoms of chaos enter even into the wave patterns associated with atomic energy levels. Starting with nuclear physics [2], one observes complexity in quantum phenomena in spectral features, eigenfunctions, dynamics of molecular processes, solid state physics and information science (Berry [4] suggested the "quantum chaology" being the adequate term for a quantum system whose classical counterpart exhibits chaos instead the mostly used and widely accepted term "quantum chaos").

Besides the quantum systems that exhibit chaos in the classical or a semiclassical limit there exists a class of quantum systems that do not have a naive classical or semiclassical counterpart. In addition, the way of passing to semiclassical approximation, e.g., in spin-boson systems is not unique and presents essential ambiguity due to different possible ways of decoupling quantum variables[5]. Different ways of performing semiclassical approximation are known to lead to different answers concerning the chaotic behaviour of the system. This ambiguity means that a classical analogue of such a model is not well-defined and cannot be a reliable object in exploring the quantum chaos issues.

The class of "spin-boson" models, e.g., two and more levels coupled to bosons (vibrons, phonons, photons) were reported to exhibit chaotic phenomena first by Lewenkopf et al [6] and Cibils et

al [8], and many others. Fujisaki et al ([9,10]) investigated the systems with the absence of a reasonable quasiclassical limit. There such phenomena as quantum tunneling and multi-mode nonadiabatic fluctuations lead to complicated wave packet dynamics which breaks down the Born-Oppenheimer adiabatic approximation.

Typical representative of such a non-adiabatic system is the two-level molecular system coupled with two vibron modes of different symmetry against the transformation of reflection – the Jahn-Teller (JT) class of models. The chaos in JT molecules was investigated within a generalized model by Cederbaum et al in a series of papers [11]. Recently, Yamasaki et al [12] for the first time investigated a possibility of chaos in spectra of the E⊗e JT model. Their analysis was based on the approximation of the Hamiltonian by separating it into the adiabatic "Mexican hat" potential and an additional part supplemented via a parameter for a nonlinear mode coupling of a trigonal symmetry to include the effect of fluctuations and non-integrability. Thus, the nonlinearity was included via mode coupling in addition to the mean field bare part of the Hamiltonian. The authors concluded that the quantum chaos reflected itself in the Wigner level spacing distribution as a consequence of the said nonlinearity of the Hamiltonian, meanwhile for the linear part the absence of these patterns was stated.

In the light of said problems due to the absence of a reasonable quasiclassical approximation we have used an exact numerical approach to the characteristics of excited (quasi-continuum) spectra of the E⊗e JT model [13,14]. This approach differs from that by Yamasaki et al. in the following: a) we *do not* introduce an explicit nonlinearity into the initial Hamiltonian. However, its SU(2) symmetry involves an *intrinsic nonlinearity* which is revealed by the exact elimination of the electronic degrees of freedom [15]. b) We started from the E⊗$(b_1 + b_2)$ model with different coupling strengths for both modes. The rotation symmetric E⊗e model represents its particular case with equal coupling constants and thus with the symmetry of higher (rotational) symmetry group [the difference of the coupling constants in realistic systems is likely to be caused, for example, by the spatial anisotropy of crystals]. The importance of starting from the more general symmetry is evident from the nature of quantum fluctuations: namely, the variational approach to E⊗$(b_1 + b_2)$ model used for the calculation of the ground state [15] was shown to yield the largest deviations just for the rotation symmetric case. In the ground state an abrupt change of the energy at equal couplings is an artefact of the adiabatic approximation: the energy region of the quantum E⊗e model is situated within a smeared border around $\beta/\alpha = 1$ (α and β being the coupling strengths of the antisymmetric and the symmetric modes, respectively) between the "selftrapping" ($\alpha > \beta$) and "tunneling" ($\alpha < \beta$) part of the ground state of the model with broken rotational symmetry. In the smeared transition region both phases coexist and are quantum correlated (entangled) via nonlinear correlations between the modes. There the phonon-assisted (by the symmetric mode) tunneling contribution to the energy [from the admixture of two reflection symmetric levels in the excitation reflection Ansatz for the variational wave function [15]] results in the essential decrease of the ground state energy because of changing parity of the wave function by the parity reversal of the phonon 1-coordinates by the operator R, $Rb_1 = -b_1R$, $\beta\langle\Psi_0^+|\hat{Q}_2R|\Psi_1{}^-\rangle = \beta\langle\Psi_0^+|\hat{Q}_2|\Psi_1^+\rangle \gg \beta\langle\Psi_0^+|\hat{Q}_2|\Psi_1{}^-\rangle$. Therefore, it has its consequence in a dramatic increase of the Ham factor and in the corresponding decrease of the energy.

Excited states follow the structure of dominating selftrapping (α) or tunneling (β) interactions. The mixing of the phases due to the tunneling is amplified by the analogous to the above matrix element via the reflection change of the parity in matrix elements with excited wave functions. Respective decrease of the energy manifests itself in the avoiding of the excited energy levels.

The phase transition at $\alpha = \beta$ to the rotational symmetry phase provides a representation by the additional rotational quantum number j. At given j in E⊗e model the analogous phonon assisted tunneling between adjacent excited levels occurs and is responsible for the flip (kink) be-

tween the levels (this mechanism can be well recognized, e.g., in Fig. 1b). This nonlinear effect causes a mixture of the adjacent (even and odd) levels at stronger couplings and leads to the nucleation of the new kink lattice phase with increasing coupling constant. The tunneling mechanism due to short-range quantum fluctuations at large j is then the origin of peculiarly irregular behaviour of the related level spacing distributions and does not allow for full developing of the Wigner chaos. The phonon assisted tunneling and nucleation of the kink lattice phase can be also demonstrated within the formalism of a Calogero-Moser gas of pseudo-particles with repulsive interaction [19].

2. Hamiltonian approach: two-level-two-boson Hamiltonians

The aim of this Section is to explore the numerical solution of the E⊗e Hamiltonian for the excited energy spectrum and wave functions in search for the statistical evidences of the symptoms of chaotic behaviour at the quantum level. Namely, the participation ratios, spectral entropies and widths of level curvature distributions are anticipated to provide the relevant indications thereof.

The E⊗e Hamiltonian with the parameter of nonintegrability α is written as

$$H = (b_1^\dagger b_1 + b_2^\dagger b_2 + 1)I + \alpha(b_1^\dagger + b_1)\sigma_z - \alpha(b_2^\dagger + b_2)\sigma_x, \quad (1)$$

where σ_j are Pauli matrices, I is the unit matrix. The pseudospin notation is used for the representation of a two-level one-electron (spinless) system.

For the secular equations of the vibronic parts of the *gerade* solution $K = +1$ ($j - 1/2 = 0, 2, 4, 6, \ldots; -2, -4, \ldots$) the representation of radial coordinates

$$H_r f_i + \frac{1}{2r^2}\left(j + \frac{1}{2}(-1)^i\right)^2 f_i + \alpha\sqrt{2} r f_k = E f_i, \quad i \neq k,\ i,k = 1,2 \quad (2)$$

$$H_r = -\frac{1}{2r}\frac{\partial}{\partial r}\left(r\frac{\partial}{\partial r}\right) + \frac{1}{2}r^2 \quad (3)$$

will be used, and radial wave functions are assumed in the form $f = \sum c_n \Phi_n$, where

$$\Phi_n = \begin{cases} \Phi^+(n_r, j, r), & n = 2n_r\,, \\ \Phi^-(n_r, j, r), & n = 2n_r + 1\,. \end{cases} \quad (4)$$

The only non-zero off-diagonal elements are

$$f_{n_r n_r} \equiv \sqrt{2}\int \Phi^+_{n_r}\Phi^-_{n_r} r \cdot r dr = \sqrt{2}\sqrt{n_r + 1 + \left|j - \frac{1}{2}\right|}, \quad (5)$$

$$f_{n_r+1 n_r} \equiv \sqrt{2}\int \Phi^+_{n_r+1}\Phi^-_{n_r} r \cdot r dr = -\sqrt{2}\sqrt{n_r + 1}\,. \quad (6)$$

The secular equations are written in the usual tridiagonal form ($E^{(0)}$ is the "unperturbed" energy for corresponding n, j),

$$\begin{aligned} c_n E_n^{(0)} + \alpha(c_{n+1} f_{n_r n_r} + c_{n-1} f_{n_r n_r - 1}) &= E c_n, \\ n &= 2n_r\,, \\ c_n E_n^{(0)} + \alpha(c_{n-1} f_{n_r n_r} + c_{n+1} f_{n_r+1 n_r}) &= E c_n, \\ n &= 2n_r + 1\,. \end{aligned} \quad (7)$$

Numerical solutions of (7) for the spectra and corresponding wave functions are exemplified in Figs. (1-4).

3. Statistical methods: Level spacing and level curvature probability distributions, long-range statistics

The multitude of avoided crossings of energy levels is generally claimed to be a testimony of quantum chaos. The fundamental problem of the quantum-mechanical manifestation of classical chaotic motion was investigated by statistical methods based on the random matrix theory (RMT). It setforth reference patterns to which the presumably quantum chaotic systems should conform [2,16]. The conventionally adopted statistical measures are either the short- or long-range statistics. The common representative of the former is the distribution of nearest neighbour level spacings (NNS), as well as the statistics involving the "curvatures" $K \equiv d^2E_n/d\alpha^2$ as functions of the nonintegrability parameter α. Among the latter a generally adopted tool is the Δ_3-statistics [16]. Both short- and long-range statistical measures have reference formulas provided within the frames of the RMT. Thus,

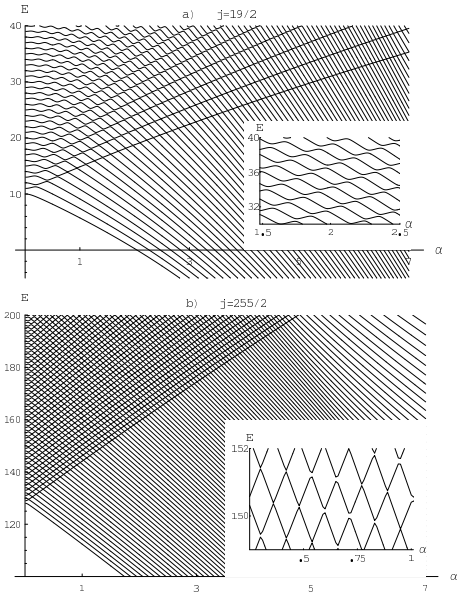

Figure 1. Energy spectra for $j = 19/2, 255/2$ as function of α.

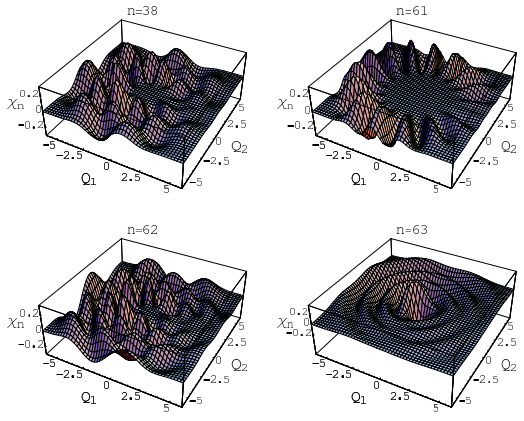

Figure 2. Numerical wavefunctions χ_n in the plane $Q_1 \times Q_2$, $\alpha = \beta = 2$. States n=61, 63 are localized ("exotic").

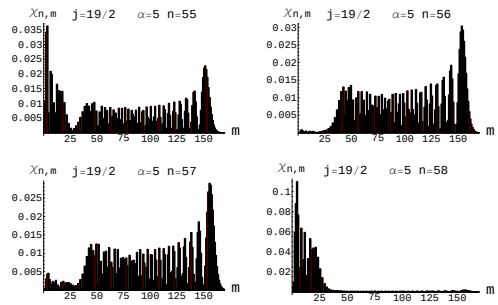

Figure 3. Projections of exact symmetric ($\beta = \alpha$) states χ_n on the harmonic oscillator base, $\chi_{n,m} = |\langle \chi_n | \Phi^0_m \rangle|^2$.

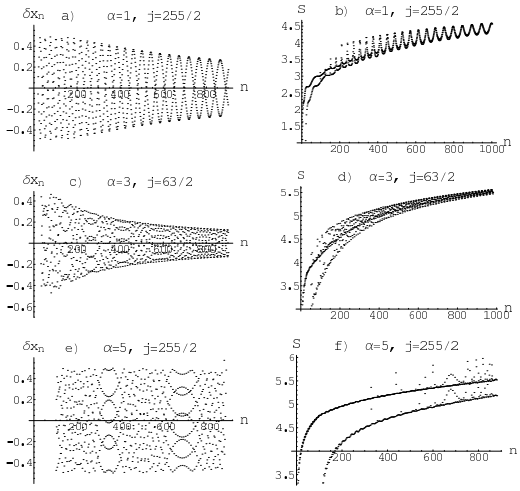

Figure 4. Reduced energies and spectral entropies of wavefunctions χ_n for different couplings α and j.

for the distribution of NNS the prediction for the fully developed chaos is the Wigner surmise $P(S) \sim S\exp(-S^2)$, for the opposite situation of the regular NNS distribution the Poisson distribution is representative $P(S) = \exp(-S)$ (in the above formulas the spectra are supposed to be scaled so that $\langle S\rangle = 1$ locally). The RMT leads to the indication of universality of level fluctuations conditioned solely by the time-reversal symmetry of the underlying Hamiltonians: the fluctuation patterns show a transition from the Poisson type to the Gaussian (orthogonal, unitary, symplectic) type as the corresponding classical system shifts from the integrable to the chaotic regime.

3.1. Spin one-boson model

The class of non-integrable spin-boson models is known to exhibit quantum chaotic symptoms for one-boson many-level ($2j+1, j = 1/2, 3/2, ...$) cases. Respective Hamiltonian

$$\begin{aligned} \hat{H} &= \omega b^\dagger b + \omega_0\sigma_z + \lambda[\sigma_+ b + \sigma_- b^\dagger + \\ &\quad \epsilon(\sigma_+ b^\dagger + \sigma_- b)]\,, \\ \sigma_\pm &= \sigma_x \pm \sigma_y \end{aligned} \tag{8}$$

is parametrized by the nonintegrability parameter ϵ. For $\epsilon = 1$ we obtain the exciton (Holstein) model (non-integrable, with evidence for chaos [5]-[8]), while for $\epsilon = 0$ one arrives at the Jaynes-Cummings model which is integrable.

3.2. E⊗(b_1+b_2) and E⊗e Jahn-Teller Model

If $\alpha \neq \beta$ but $|\alpha - \beta| \ll \alpha$ in (1), there appear correlations between the excited levels with $j \neq j'$ of the Hamiltonian in radial representation due to the term [13]

$$(\alpha - \beta)\sqrt{2}r \cdot \begin{pmatrix} \sin\phi R_{ph} & 0 \\ 0 & -\sin\phi R_{ph} \end{pmatrix}. \tag{9}$$

Respective additional avoided level crossings change dramatically the probability distributions of level spacings when compared to those of the $E \otimes e$ model ($\alpha = \beta$), Fig. 5.

Fig. 5 presents the typical forms of the NNS distributions for different α, β of the JT model with broken radial symmetry. It is seen that for the special cases of higher symmetry the NNS distributions indeed are close to the Poisson distribution (first row). Meanwhile far from the

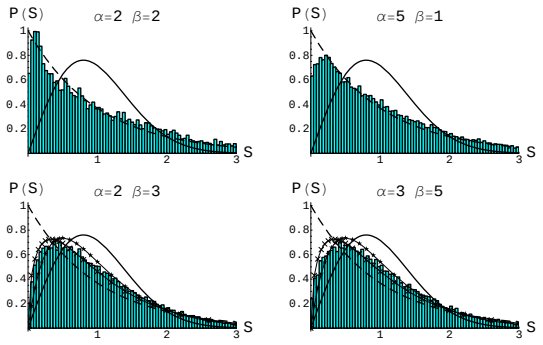

Figure 5. Sample nearest-neighbor distributions of levels (unfolded and scaled to $\langle S\rangle = 1$) for different values of α, β. The curves on the histograms represent Poisson (long dashed), Wigner (full), semi-Poisson (stars) and $\sqrt{S}$ (crosses) distributions.

cases $\alpha = \beta$ and $\alpha \ll \beta$, $\alpha \gg \beta$ the NNS distributions do not show a tendency to the RMT prediction (Wigner surmise). The well defined limit for these distributions seems not to have an analogue in the present versions of the RMT ensembles and presents some intermediate statistics about which we can make now only plausible assumptions. Thus, it is found that the semi-Poisson distribution $P(S) = 4S\exp(-S)$ [17,18] describes well this intermediate statistics in the domain of large $S \geq 1$ although for small S the limiting distribution seems to scale as $P(S) \sim S^\nu$ with ν ranging between $0.3 \div 0.5$. The semi-Poisson statistics has recently found its application as a limiting case of level statistics at the M-I transition in Anderson localization models and, therefore, such an analogy seems to be a promising item. As the second fitting formula (see Fig. 5, second row) we use the $\sqrt{S}$-distribution $P(S) \sim \sqrt{S}\exp(-3/2S)$ which conforms to the interpolation of Brody type. From the numerical analysis of the nearest-neighbour level spacing probability distributions $P(S)$ we conclude the diagnosis of the quantum chaotic patterns of JT models:

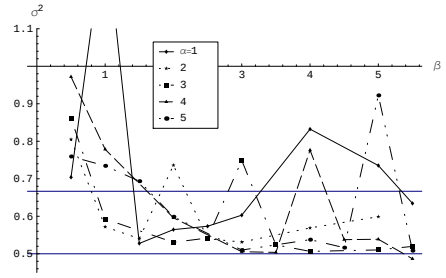

Figure 6. Standard deviations $\sigma^2 = \langle S^2 \rangle - 1$ of the NNS distributions. Grid lines correspond to the semi-Poisson (0.5) and $\sqrt{S}$ (2/3) values. Far from the higher symmetry cases (Holstein and E⊗e JT model) the dispersion tends to a *well defined limit* $\sigma^2 \simeq 0.5$. The fully chaotic Wigner NNS distribution would have $\sigma^2 \simeq 0.28$.

1. For small S, $P(S) \sim S^\nu$, where ν acquires a non-universal value from the interval $(0.3, 0.5)$.

2. Except for small S, the limit cases of $E \otimes (b_1 + b_2)$ model of higher symmetry (E⊗e and Holstein) show up the close-to-Poisson distribution of NNS, especially in tails (Fig. 5, first row).

3. Far from the higher symmetry cases the NNS distribution tends to a universal law which is however markedly distinct from the Wigner distribution expected for the fully developed quantum chaos (Fig. 5, second row).

4. The dispersion tends to a *well defined and universal limit* $\sigma^2 \simeq 0.5$ (Fig. 6) referring to the semi-Poisson distribution $P(S) = 4S\exp(-2S)$. This distribution is known as a critical distribution at the M-I transition in Anderson localization models.

For the $E \otimes e$ model a more pronounced indication for the presence of quantum chaos than the NNS level spacing distribution is the conventionally adopted [20] linear scaling behaviour of the widths of curvature probability distributions

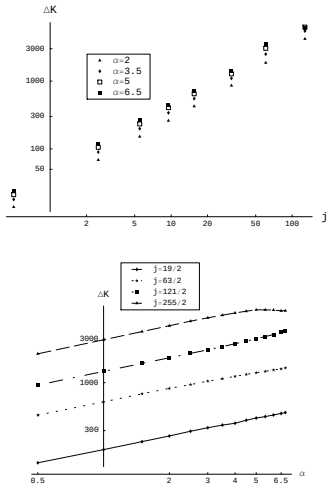

Figure 7. The widths of curvature distributions $\Delta K \equiv \langle \Delta^2 K \rangle$ as function of j (a) and α (b). The scaling laws $\Delta K \sim j^\nu$ and $\Delta K \sim \alpha^\nu$ are seen.

$\Delta K \equiv \langle \Delta^2 K \rangle$ as a function of nonintegrability parameter (α), Fig. 7. The quantum number j is a measure of a departure from the semiclassical limit $j \to \infty$. From Fig. 8 it is seen that the widths of the curvature distribution show a scaling $\Delta K \sim j^\mu \alpha^\nu$ with $\mu \simeq 1$ and $\nu \simeq 0.5$. The latter observation, as well as the form of the typical profiles of $P(K)$ allows for the interpretation of the evolution of $P(K)$ in the pseudo-time α as a solution of an ordinary diffusion-like equation with added ballistic ("telegraph") term $d^2P(K)/d\alpha^2$ [7]. For comparison with the level clustering (dimerization) found in one-boson spin models ([8,21]) it is interesting to demonstrate the numerical evidence of the trimerization in the $E \otimes e$ model. From Fig. 8 it is evident that the clustering of levels with two and three dominant spacings at fixed angular momenta causes notable deviations from both Poisson and Wigner distributions. The third (localized) peak is characteristic for the two-boson case of a two-level model, while the one-boson case is distinguished by the two peak structure. The long-range statistics comprises a characteristics of the spectrum

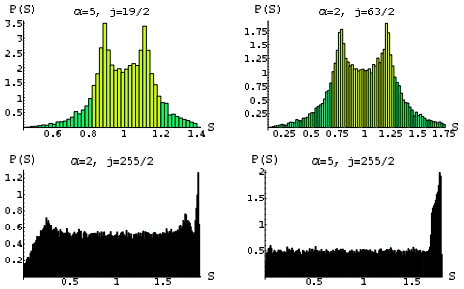

Figure 8. Level spacing distributions for particular j. Dimerization clustering related to two dominating level spacings is evident for $\alpha = 2$ and $j = 63/2$; Third peak from localized states occurs at large j and α, dominating close to the semiclassical limit (compare with Fig. 4). The crossover from the linear dimerized regime to the nonlinear localized regime with increasing j and α is evident.

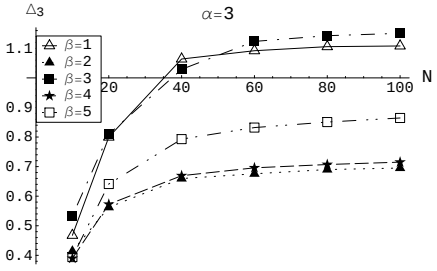

Figure 9. Example of the Δ_3-statistics (spectral rigidity) for the JT model. The long-range statistics appears to show the log-like behaviour as function of $\langle N\rangle$ typical for the RMT predictions (fully developed quantum chaos).

defined as its "rigidity measure". Among possible forms of this parameter one can name the fluctuation of level number $\delta^2 N$ in an energy band of the widths E, the Δ_3 statistics [16,17,18] etc. The RMT, in its turn, predicts a characteristic behaviour for all these measures which should scale as $\log E$ (or $\log\langle N\rangle$), meanwhile for fully uncorrelated sequences of levels the linear scaling $\sim \langle N\rangle$ is expected. In Fig.8 the sample example of the long-range statistics $\langle\Delta_3\rangle$ is given. It is seen that the behaviour of the spectral rigidity of the JT systems conforms rather to the RMT patterns.

4. Vibronic spectra of $E \otimes e$ Jahn-Teller model as a Calogero-Moser gas of pseudo-particles with repulsion.

The approach of the present section is to some extent complementary to the statistical approach of the preceding section. The mapping of energy spectra $E_n(\alpha)$ of non-integrable Hamiltonians with one parameter of non-integrability (α), $H = H_0 + \alpha V$ where H_0 is integrable, on a classical integrable Calogero-Moser model of interacting pseudo-particles moving in a pseudo-time α is a very useful tool for investigation of energy spectra of non-integrable systems first introduced by Pechukas and Yukawa [19]. The mapping is based on definition of the dynamic variables $E_n(\alpha) \equiv x_n(\tau)$, $dx_n/d\tau = p_n(\tau)$, with the pseudo-time $\tau \equiv \alpha$. Respective classical dynamic equations for pseudo-particles evolving in the pseudo-time τ with repulsive interactions can be rewritten for fluctuations δ_{2n} defined as $x_{2n+1} - x_{2n} = 1 + \delta_{2n}$. The Calogero-Moser set of equations reads

$$\frac{dp_n}{d\tau} = 2\sum_{m(\neq n)} \frac{L_{nm}L_{mn}}{(x_m - x_n)^3}$$

$$\frac{dL_{mn}}{d\tau} = \sum_{l\neq(m,n)} L_{ml}L_{ln}\left[\frac{1}{(x_n - x_l)^2} - \frac{1}{(x_m - x_l)^2}\right], \quad (10)$$

where

$$\begin{aligned} L_{mn}(\tau) &= (x_n(\tau) - x_m(\tau))\cdot V_{mn} = -L_{nm} \\ p_n &\equiv \langle n(\tau)|V|n(\tau)\rangle \equiv V_{nn}\,. \end{aligned} \quad (11)$$

V_{mn} are matrix elements of the Hamiltonian. Special case is the Hamiltonian with excited spectrum consisting of 2×2 diagonal clusters with diagonal and nearest neighbor off-diagonal elements, $f_{n_r n_r} \equiv= f_{d n_r}$ and $f_{n_r+1,n_r} \equiv f_{o n_r+1}$, respectively. For the case (7) we have $V_{2n+1,2n} = f_{d n_r}$, $V_{2n,2n-1} = f_{o n_r}$. There is

$L_{2n+12n} = f_{d n_r}(x_{2n+1}(\tau) - x_{2n}(\tau))$,

$$f_{d_{n_r}} = 2\sqrt{2}\sqrt{n+1+|j-1/2|},$$
$$L_{2n-12n} = f_{o_{n_r}}(x_{2n}(\tau) - x_{2n-1}(\tau)),$$
$$f_{o_{n_r}} = -\sqrt{2}\sqrt{n}\,. \qquad (12)$$

For what follows we define small fluctuation δ by $x_{2n+1} - x_{2n} \equiv 1 + \delta_{2n}$, and approximate $(x_{2n+1} - x_{2n})^{-1} \approx 1 - \delta_{2n} + \delta_{2n}^2 - \delta_{2n}^3$. Then, for energy fluctuations δ_{2n}, δ_{2n+1} from (7), (10) and (12) we get nonlinear equations with the lowest powers of nonlinearity in the form

$$\frac{\partial^2\bar{\delta}_{2n+1}}{\partial\tau^2} - 4f_{d_{n_r+1}}^2(\bar{\delta}_{2n+2} + \bar{\delta}_{2n} - 2\bar{\delta}_{2n+1}) = 8(f_{d_{n_r+1}}^2 - f_{o_{n_r+1}}^2)\bar{\delta}_{2n+1} - 4(f_{d_{n_r+1}}^2 - f_{d_{n_r}}^2)\bar{\delta}_{2n} - 8f_{o_{n_r+1}}^2\bar{\delta}_{2n+1}^2 + 4f_{d_{n_r+1}}^2\bar{\delta}_{2n+2}^2 + 4f_{d_{n_r}}^2\bar{\delta}_{2n}^2 + +O(\bar{\delta}^3)\,, \qquad (13)$$

$$\frac{\partial^2\bar{\delta}_{2n}}{\partial\tau^2} - 4f_{o_{n_r+1}}^2(\bar{\delta}_{2n+1} + \bar{\delta}_{2n-1} - 2\bar{\delta}_{2n}) = 8(f_{o_{n_r+1}}^2 - f_{d_{n_r+1}}^2)\bar{\delta}_{2n} - 4(f_{o_{n_r+1}}^2 - f_{o_{n_r}}^2)\bar{\delta}_{2n-1} - 8f_{d_{n_r}}^2\bar{\delta}_{2n}^2 + 4f_{o_{n_r+1}}^2\bar{\delta}_{2n+1}^2 + 4f_{o_{n_r}}^2\bar{\delta}_{2n-1}^2 + O(\bar{\delta}^3). \qquad (14)$$

Eqs. (13) and (14) can be approximated by taking second terms on the l.h.s. as second derivatives. In view of definitions (12) for large $j \gg n$ we have $|f_{o_{n_r+1}} < |f_{d_{n_r}}|$, $f_d(n_r+1) \approx f_{d_{n_r}}$. If we redefine $\bar{\delta}_{2n} = \delta_{2n} - 1$ and assume for the deviations plausible relations $\bar{\delta}_{2n}^2 \approx \bar{\delta}_{2n+2}^2 \approx \bar{\delta}_{2n+1}^2$ in Eq. (13) and (14), we obtain, up to the second order

$$\frac{\partial^2\bar{\delta}_{2n+1}}{\partial\tau^2} - 4f_{d_{n_r+1}}^2\frac{\partial^2\bar{\delta}_{2n+1}}{\partial n^2} \approx 8f_{d_{n_r+1}}^2(\bar{\delta}_{2n+1} + \bar{\delta}_{2n+1}^2), \qquad (15)$$

$$\frac{\partial^2\bar{\delta}_{2n}}{\partial\tau^2} - 4f_{o_{n_r+1}}^2\frac{\partial^2\bar{\delta}_{2n}}{\partial n^2} \approx -8f_{d_{n_r}}^2(\bar{\delta}_{2n} + \bar{\delta}_{2n}^2). \qquad (16)$$

In view of different signs of the potentials on the r.h.s. of equations (15) and (16) even and odd pseudo-particles can be related as moving in real and imaginary space, $\tau \to i\tau$, $n \to in$, respectively.

Analogously, alternative set of equations reads

$$\frac{\partial^2\bar{\delta}_{2n+1}}{\partial\tau^2} - 4f_{o_{n_r+1}}^2\frac{\partial^2\bar{\delta}_{2n+1}}{\partial n^2} \approx 8f_{d_{n_r+1}}^2(\bar{\delta}_{2n} + \bar{\delta}_{2n}^2), \qquad (17)$$

$$\frac{\partial^2\bar{\delta}_{2n}}{\partial\tau^2} - 4f_{d_{n_r}}^2\frac{\partial^2\bar{\delta}_{2n}}{\partial n^2} \approx -8f_{d_{n_r+1}}^2(\bar{\delta}_{2n+1} + \bar{\delta}_{2n+1}^2). \qquad (18)$$

Transition to the imaginary space changes the sign of the potential, i.e. the particle turns to the tunneling domain and the pseudo-particles change their parity, e.g. $\bar{\delta}_{2n+1}(v_1 \equiv 2f_{d_{n_r}} \to \bar{\delta}_{2n}(v_1)$, $\bar{\delta}_{2n}(v_2 \equiv 2f_{d_{n_r}} \to \bar{\delta}_{2n+1}(v_2 \equiv 2f_{o_{n_r+1}})$, so that the trajectories interchange their velocities, $\bar{\delta}_{2n}(v_2) \equiv 2f_{o_{n_r+1}} \to \bar{\delta}_{2n}(v_1) \equiv 2f_{d_{n_r}}$ and $\bar{\delta}_{2n+1}(v_1 \equiv 2f_{d_{n_r}} \to \bar{\delta}_{2n+1}(v_2) \equiv 2f_{o_{n_r+1}}$. By another words, the particles interchange their velocities, v_1, v_2 when transferring from real to imaginary space and vice versa. This scenario can be understood as series of soliton collisions related to two subsequent levels.

Indeed, equation (15) for large j ($f_{d_{n_r+1}} \sim 2\sqrt{|2j-1|}$) admits solution in form of the propagating nonlinear pulse $\bar{\delta}(\zeta = n - v\tau)$

$$\bar{\delta}_{2n+1}(\zeta - \zeta_0) = -\frac{3}{2}\cosh^{-2}\left(\frac{\zeta - \zeta_0}{L}\right), \qquad (19)$$

where $\zeta_0 = n_0 - v\tau_0$ restores the translational invariance in the system of levels and $L = (v^2 - (f_{d_{n_r+1}})^2)^{1/2}/[2\sqrt{2}|f_{d_{n_r+1}}|]$ is the soliton width. The corresponding coordinate is identified from $\partial x_{2n+1}/\partial n = 1 + \delta_{2n+1}$ as a soliton (kink) solution

$$x_{2n+1} = 2n - \frac{3L}{2}\tanh\left(\frac{\zeta - \zeta_0}{L}\right). \qquad (20)$$

If in equations (15) and (16) one approximates $\bar{\delta}_{2n+2} \approx \bar{\delta}_{2n}$ and assumes $\bar{\delta}_{2n+1} = -\bar{\delta}_{2n}$ one obtains approximately

$$\delta_{2n+1} \approx -\frac{f_{d_{n_r+1}}^2 + f_{d_{n_r}}^2}{2f_{o_{n_r+1}}^2}\delta_{2n}(1 - \delta_{2n}). \qquad (21)$$

Equation (21) is a well known logistic equation implying transition to the chaotic regime for $A = \frac{f_{d_{n_r+1}}^2 + f_{d_{n_r}}^2}{2f_{o_{n_r+1}}^2} \sim \frac{n+|j-1/2|}{n} \geq A_{crit} = 3.56994\ldots$.

Conventionally, the term "quantum chaos" is

used to denote the traces of *classical* chaotic behavior at a quantum level. As already mentioned in the Introduction, the classical counterpart of the system under consideration cannot be defined uniquely. The semiclassical approximation in two-level systems generically leads to classical chaotic patterns as a result of nonlinear coupling between two subsystems, boson and electron, considered respectively as classical and quantum; The onset of classical chaos corresponds to the energies above the first diabatic line. It is to be emphasized that the mentioned chaotic behavior refers to purely quantum regime of medium j and n_r between the weak coupling with $j \ll n_r$ (dimerized pairs of oscillators) and strong coupling with $j \gg n_r$ (kink lattice) domains. Thus, this chaotic behavior can be regarded as being of essentially quantum nature. One can conclude, that the mapping of the quantum system on the classical Calogero-Moser gas with repulsive interactions enables one to use the classical formalism for describing the system via its quantum numbers. So the remarkable feature of this approach is its ability to represent quantum chaos by classical equations.

5. Acknowledgments

The support of the project by the Grant Agency of the Czech Republic No. 202/06/0396 is greatly acknowledged. Partial support is acknowledged also from the project No. 2/6073/26 of the Grant Agency VEGA, Bratislava.

REFERENCES

1. M. C. Gutzwiller, *Chaos in Classical and Quantum Systems (Springer-Verlag, New York,1990).*
2. B. Eckhardt, Phys. Rep. **163**, 205 (1988).
3. K. Nakamura, Quantum Chaos-A New Paradigm of Nonlinear Dynamics (Cambridge University Press, Cambridge, 1993).
4. M. V. Berry, Proc. R. Soc. London, Ser. A **413**, 183 (1987).
5. R. Graham and M. Hörnerbach, Z. Phys. B **57**, 233 (1984), R. Graham and M. Hörnerbach, Phys. Lett. 101A, 61 (1984).
6. C.H. Lewenkopf, M.C. Nemes, V. Marvulle, M.P. Pato and W.F. Wreszinski, Phys. Lett. A **155** 113 (1991).
7. V. V. Uchaikin, Physics-Uspekhi 46, 821 (2003).
8. M. Cibils, Y. Cuche, G. Müller, Z. Physik, **97**, 565 (1995).
9. H. Fujisaki, Phys. Rev. E **63** 066221 (2001).
10. H. Fujisaki, Phys. Rev. A **70** 012313 (2004).
11. E. Haller, H. Köppel, and L.S. Cederbaum, Chem.Phys.Lett **101**, 215 (1983); Th. Zimmerman, H. Köppel, and L.S. Cederbaum, J. Chem. Phys. **91**, 3934 (1989).
12. H. Yamasaki, Y. Natsume, A. Terai, K. Nakamura, Phys. Rev. **E 68**, 0462011 (2003).
13. E. Majerníková, S.Shpyrko, Phys. Rev. E **73** 066215 (2006); e-print:cond-mat/0509687.
14. E. Majerníková, S.Shpyrko, Phys. Rev. E **73** 057202 (2006); e-print:cond-mat/0510710.
15. E. Majerníková and S. Shpyrko, J. Phys.: Condens. Matter **15**, 2137 (2003).
16. M. L. Mehta, Nucl.Phys. **18**, 395 (1960); M. L. Mehta, M. Gaudin, Nucl.Phys. **18**, 420 (1960); M. Gaudin, Nucl. Phys. **25**, 447 (1961).
17. S. N. Evangelou, J.-L. Pichard, Phys. Rev. Lett. **84**, 1643 (2000); S. N. Evangelou, D. E. Katsanos, Phys. Lett.**A 334**, 331 (2005); E. B. Bogomolny, U. Gerland, C. Schmit, Phys.Rev.E **59**, R1315 (1999).
18. B.I.Shklovskii, B.Shapiro, B.R.Sears, P.Lambrianides, H.B.Shore, Phys.Rev.B **47**, 11487 (1993).
19. P. Pechukas, Phys. Rev. Lett. **51**, 943 (1983); T. Yukawa, Phys. Lett. **A 116**, 227 (1986).
20. K. Nakamura, Y. Nakahara, A.R. Bishop, Phys.Rev.Lett **54** 861 (1985); K. Nakamura, A.R. Bishop, Phys. Rev. **B33**, 1963 (1986).
21. R. Steib, J.L. Schoendorff, H.J. Korsch and P. Reineker, Phys. Rev. E **57** 6534 (1998).